JOURNAL OF GUIDANCE, CONTROL, AND DYNAMICS
Vol. 24, No. 3, May–June 2001

Two Reconfigurable Flight-Control Design Methods: Robust Servomechanism and Control Allocation

John J. Burken*
NASA Dryden Flight Research Center, Edwards, California 93523
Ping Lu† and Zhenglu Wu‡
Iowa State University, Ames, Iowa 50011-2271
and
Cathy Bahm*
NASA Dryden Flight Research Center, Edwards, California 93523

Two methods are discussed for design of reconfigurable flight-control systems when one or more control surfaces are jammed. The first is a robust servomechanism control approach, which is a generalization of the classical proportional-plus-integral control to multi-input/multi-output systems. The second proposed method is a control-allocation approach based on a quadratic programming formulation. The formulation is formally analyzed, and a globally convergent fixed-point iteration algorithm is used to make onboard implementation of this method feasible. The two methods are applied to reconfigurable entry flight control design for the X-33 vehicle. Nonlinear six-degree-of-freedom simulations demonstrate simultaneous tracking of angle-of-attack and roll-angle commands during control surface failures. The control-allocation method appears to offer more uniform and good performance at the expense of modestly higher computation requirement.

I. Introduction

FLIGHT-CONTROL system reconfiguration is concerned with making changes in flight-control system to adapt to failures and damages. The adaptation is usually in the forms of control system gain changes or control law changes. Reconfigurable control offers the potential of significant enhancement of flight safety and mission success rate. The reconfigurable controller has the potential of landing a crippled airplane safely and thus increasing mission success rates. Because of its clear benefits in both military and civil applications, flight-control reconfiguration research has received considerable attention in recent years, exemplified by the U.S. Air Force Reconfigurable Control for Tailless Fighter Aircraft program[1] and the NASA X-33 program.[2] The references contained in Ref. 1 provide a glimpse of some previous studies on this subject. An often investigated approach for reconfigurable control system design is through some form of model-following technique, typically by means of either parameter adaptation[3] or neural networks.[1] More recently, reconfigurable control designs using dynamic inversion and neural network to adaptively cancel inversion errors have demonstrated good performance.[4]

A major task in control reconfiguration deals with adjusting the controller gains on-line or switching to a different control law to compensate for the failure. This paper focuses on this aspect. More specifically, the failure is assumed to be a jammed aerodynamic effector, which is among class 1 failures as defined in Ref. 1. It will be further assumed, when necessary, that the aircraft is fitted with smart actuators so that the jammed control surfaces can be detected and the position identified. This condition is already readily met by actuators available today.[2]

The objective of this work is to seek reconfigurable control system designs that are easily implementable in flight software, reliable, and offer a degree of assurance of success for the targeted types of failures. The reconfigured control system is expected to restabilize the aircraft should control surface jamming occur and provide reasonable command-tracking performance.

To these ends, two approaches are investigated and evaluated in this paper. One is based on the robust servomechanism design,[5,6] which is a generalization of the classical proportional-plus-integral (PI) design. In this approach the effect of the jammed surface is treated as a disturbance to the system. A PI controller is designed to stabilize the aircraft (stabilization), balance the jammed surface (disturbance rejection), and provide command tracking. The second method is developed by the authors of this paper, which is based on a control-allocation approach. Here a reference baseline control law is first designed for the healthy aircraft with all of the control surface operable. At any given state the desired control inputs (e.g., moments and forces) to the aircraft can be computed from this baseline control law. In the event of a jammed surface, the redundant degree of freedom of the control effectors is utilized to distribute the deflections of the operable surfaces in an optimal fashion so as to cancel the influence of the jammed surface and reproduce as closely as possible the desired inputs the reference controller would have produced to the aircraft.

As a demonstration, the two approaches are applied to a reconfigurable entry flight-control system design for the X-33 vehicle. The X-33 vehicle is a one-half-scale suborbital prototype single-stage-to-orbit reusable launch vehicle. In flight tests the X-33 vehicle will accelerate to approximately Mach 9 and climb to an altitude of approximately 200,000 ft. The entry flight immediately follows a short transition phase after the ascent. Figure 1 shows the configuration of the X-33. The X-33 has four sets of control surfaces: rudders, body flaps, inboard and outboard elevons, with left and right side for each set. Each of the eight surfaces can be independently actuated with one actuator for each surface. All of the aerosurfaces will use electromechanical actuators (EMAs). The body flaps also have an pneumatic load assist device that can be used for a total of 40 s during ascent or entry.

Analysis has shown that although the probability for an actuator failure is very low, when it does happen, the failure would most likely result in jam of the associated aerosurface.[2] The EMAs are capable of failure detection and identification within 120–160 ms. This capability provides information on which surface, if any, is jammed, and jammed at what position. The reconfigurable control design is

Received 22 April 1999; revision received 10 November 2000; accepted for publication 30 November 2000.

*Aerospace Engineer. Member AIAA.
†Associate Professor, Department of Aerospace Engineering and Engineering Mechanics; plu@iastate.edu. Associate Fellow AIAA.
‡Graduate Student, Department of Aerospace Engineering and Engineering Mechanics.

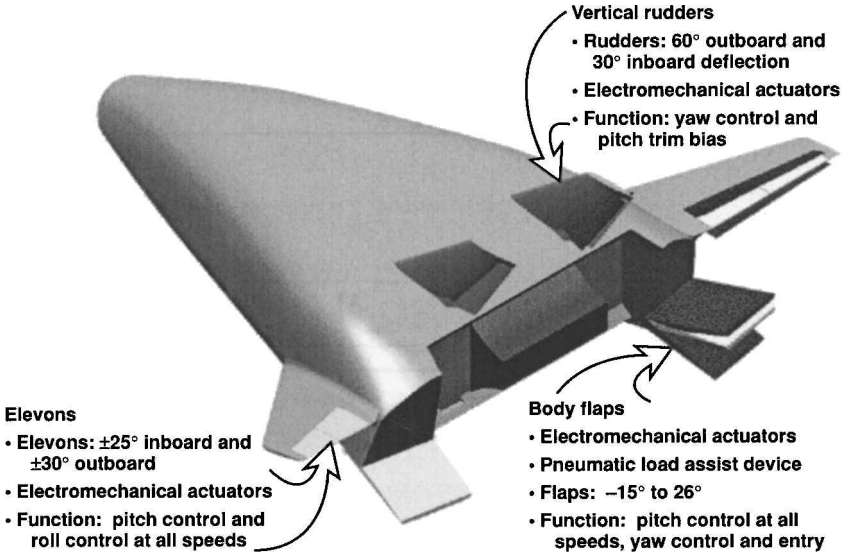

Fig. 1 X-33 advanced technology demonstrator.

done for each surface failure. The eight control surfaces have control power capable of providing redundant pitch, roll, and yaw restoring moments such that if one surface fails, the potential exists for an alternate control scheme to maintain control of the vehicle.

The control system reconfiguration problem for the X-33 is posed as follows: If a single control surface fails (jams, floats, or runs away), can the nominal or reconfigurable controller be used to land the vehicle safely? A nominal controller has some inherent robustness and may be able to handle a limited failure set (such as a left rudder jammed at 3 deg). An appropriately designed reconfigurable controller should have a much larger region of survivable failure conditions. The two proposed reconfigurable control designs appear to meet this challenge well.

The methodology for the robust servomechanism design is reviewed in Sec. II. In Sec. III, the control-allocation method is introduced as a quadratic programming (QP) problem; two analytical yet practically useful properties of this formulation are established; and a globally convergent fixed-point iteration algorithm suitable for onboard implementation is described. Section IV contains the application of the two methods to reconfigurable entry flight control of the X-33 vehicle and the evaluation of the performance. Conclusions are given in Sec. V.

II. Servomechanism Problem for Multi-Input/Multi-Output Systems

The servomechanism problem is concerned with control of a dynamic system to achieve asymptotic tracking of desired output and rejection of unmeasurable disturbance. For single-input/single-output (SISO) systems the problem has been well understood for 50 years. However, it is only in the last two decades that this problem has been solved for multi-input/multi-output (MIMO) systems. In the following a simpler version of the problem is introduced, and the controller design methodology is reviewed. For more complete discussion and detail the reader is referred to Refs. 5 and 6.

A. Problem Formulation

Consider a linear, time-invariant, MIMO system:

$$\dot{x} = Ax + Bu + Ew \tag{1}$$

$$y = Cx + Du + Fw \tag{2}$$

where $x \in R^n$ is the plant state, $u \in R^m$ the plant input, $w \in R^l$ the disturbance, and $y \in R^p$ the controlled output with $p \leq m$. Let $r \in R^p$ represent the desired history for y. Assume further that r and w are modeled by

$$r^{(q)} + \alpha_1 r^{(q-1)} + \cdots + \alpha_{q-1}\dot{r} + \alpha_q r = 0 \tag{3}$$

$$w^{(q)} + \alpha_1 w^{(q-1)} + \cdots + \alpha_{q-1}\dot{w} + \alpha_q w = 0 \tag{4}$$

with $q \geq 1$. The preceding formulation encompasses many commonly used signals, including constants (when $q = 1$ and $\alpha_1 = 0$), polynomials (when $\alpha_i = 0, i = 1, \ldots q$), sinusoidal functions (when $q = 2$, $\alpha_1 = 0$, and $\alpha_2 > 0$) and exponential functions. The initial conditions for w are assumed to be arbitrary; therefore, $w(t)$ is considered unknown (unmeasurable). In a more general formulation the dynamics of $r(t)$ and $w(t)$ do not have to be the same.[6] But they are assumed to be the same here for simplicity, and such an assumption is adequate for our specific purpose in this paper. The objectives of the control design are to find a feedback controller such that 1) the closed-loop system is stable; 2) the error $e(t) = r(t) - y(t)$ approaches zero in the presence of the unmeasurable (possibly time-varying) disturbance $w(t)$; and 3) the closed-loop system is robust in the sense that asymptotic tracking of r and rejection of w are maintained in the presence of system parametric uncertainty or even variations in the order of the dynamics, as long as the closed-loop system remains stable.

B. Robust Servomechanism Design Methodology

A dynamic controller is to be designed to meet the objectives just stated. The controller dynamics are set to be

$$\dot{x}_c = A_c x_c + B_c(r - y) \tag{5}$$

where $x_c \in R^{pq}$ is the controller state and $A_c \in R^{pq \times pq} = \text{block diag}[\Gamma, \ldots, \Gamma]$ with

$$\Gamma = \begin{bmatrix} 0 & 1 & 0 & \cdots & 0 \\ 0 & 0 & 1 & \cdots & 0 \\ \vdots & \vdots & \vdots & \vdots & \vdots \\ 0 & 0 & \cdots & 0 & 1 \\ -\alpha_q & -\alpha_{q-1} & \cdots & -\alpha_2 & -\alpha_1 \end{bmatrix} \in R^{q \times q} \tag{6}$$

and $B_c \in R^{pq \times p} = \text{block diag}[\gamma, \ldots, \gamma]$ with

$$\gamma = \begin{bmatrix} 0 \\ \vdots \\ 0 \\ 1 \end{bmatrix} \in R^q \tag{7}$$

Consider the open-loop system including the plant [Eq. (1)] and the controller dynamics [Eq. (5)] with $r = 0$

$$\begin{bmatrix} \dot{x} \\ \dot{x}_c \end{bmatrix} = \begin{bmatrix} A & 0 \\ -B_c C & A_c \end{bmatrix} \begin{bmatrix} x \\ x_c \end{bmatrix} + \begin{bmatrix} B \\ -B_c D \end{bmatrix} u \tag{8}$$

Let $\lambda_1, \ldots, \lambda_q$ be the roots of the polynomial

$$\lambda^q + \alpha_1 \lambda^{q-1} + \cdots + \alpha_{q-1}\lambda + \alpha_q = 0$$

Suppose that the following condition is satisfied:

$$\text{rank} \begin{bmatrix} \lambda_i I - A & B \\ -C & D \end{bmatrix} = n + p, \qquad i = 1, \ldots, q \tag{9}$$

then the augmented system (8) is controllable.[5,6] Hence there exist control laws

$$u = kx + k_c x_c \tag{10}$$

such that the closed-loop system is stable. Furthermore, when $r \neq 0$ and satisfies Eq. (3), asymptotic tracking and disturbance rejection are achieved by such a control law. That is, $e = r - y \to 0$ for any initial condition $x(0)$ and any w satisfying Eq. (4). The closed-loop system possesses robustness in the sense that for any (not necessarily small) perturbations in $\{A, B, C, D, B_c, k, k_c\}$, asymptotic tracking and disturbance rejection still hold as long as the closed-loop system remains stable and B_c remains block diagonal.[5,6]

Remarks:

1) Because the augmented system (8) is controllable, the control law (10) can be conveniently found by applying the linear quadratic regulator (LQR) approach to Eq. (8).

2) In the special case where r is constant command and w is constant (but possibly unknown) disturbance, we have $q = 1$ and $\alpha_1 = 0$; therefore, $A_c = 0$, and $B_c = I_{p \times p}$ according to their definitions. From the controller dynamics (5) it can be seen that $x_c = \int (r - y)\, dt = \int e\, dt$. Thus the control law (10) is simply a PI control law, which is well known in classical SISO control theory. But the current formulation is much more general in that it applies to MIMO systems and allows tracking of time-varying commands and rejection of time-varying disturbances.

3) The principle of this class of methods is also alternatively known as the internal model principle in the literature because the controller has to include the models of the disturbance and command in order to achieve disturbance rejection and command tracking.

4) This robust servomechanism design applies conveniently to control of impaired aircraft with one or more jammed control surfaces. Suppose that the dynamic model (1) represents the linearized dynamics of such an aircraft at a trim condition. Let w in Eq. (1) denote the (constant) position of the jammed surface and u all of the remaining operable surfaces. The exact value of w does not need to be known with this method. The matrix E (a column vector in this case) in Eq. (1) is then the stability derivative associated with the surface now jammed (i.e., the column corresponding to the jammed surface in the B matrix of the linearized model prior to failure). Now the problem is cast into the formulation in Sec. II.A and a PI controller (10) can be designed by LQR or pole-placement methods to stabilize the aircraft, reject the influence of the jammed surface, and track constant commands.

III. Control Reconfiguration via Control Allocation

Control allocation is concerned with how to distribute the deflections of multiple control surfaces of the aircraft to generate required control inputs (pitch, roll, and yaw moments, and forces) when the number of the control surfaces is greater than the number of required control inputs. Reference 7 contains a list of recent work on control allocation and provides exploratory discussions to several control allocation approaches based on quadratic and linear programming. In this section we consider a control reconfiguration approach, also based on a control allocation scheme using the QP method. The idea is to use the redundancy of the operable control surfaces to cancel the effects of the jammed surface and still provide the same (or almost the same) desired control inputs. Clearly the greater the control redundancy is, the better suited this approach would be. Also, this approach will require the position of the jammed surface to be known, either through the use of smart actuator or by estimation.

A. Problem Formulation

Let the linearized dynamics of the normal aircraft at a trim condition be given by

$$\dot{x} = Ax + Bu \tag{11}$$

It is assumed that a reference control law has been designed based on the model (11) that provides satisfactory stabilization and command-tracking performance for the aircraft. Suppose now that one of the control surfaces is suddenly jammed at a position w. Rewrite the postfailure state equation of the system (11) as

$$\dot{x} = Ax + B_r u_r + d_x \tag{12}$$

where $u_r \in R^m$ represents the remaining control surfaces, B_r the postfailure control influence matrix, $d_x = b_w w$ is the input to the aircraft caused by the jammed surface w, where b_w is the column in B corresponding to the jammed surface. Note that d_x is known when w is known. Let $z = C_z x$ be a selected i-dimensional controlled output vector ($z \in R^i$) to be used in defining the control allocation. From Eq. (12) and the definition of z we have

$$\dot{z} = C_z Ax + C_z B_r u_r + C_z d_x \triangleq A_z x + B_z u_r + d_z \tag{13}$$

The choice of z is not necessarily the same as y in Sec. II, but must be one such that the closed-loop stability and performance can be ensured from control of z. From a control theoretical viewpoint the closed-loop stability requirement implies that the choice of the controlled output z should lead to a nonminimum-phase system. One most natural choice of z is $z = (p\ r\ q)^T$ (the roll, yaw, and pitch rates). Other choices are also possible. We require in general that $m \geq i$ in this approach (i.e., the number of operable control surfaces is greater than that of the controlled variables). At the current state $x(t)$ suppose that the reference baseline feedback control law for the healthy aircraft would have produced input $u^* \in R^{m+1}$ if all of the control surfaces were operable. Then the desired rate of z would be

$$\dot{z}^* = C_z Ax + C_z Bu^* \tag{14}$$

We seek a u_r that makes the right-hand side of Eq. (13) as close as possible to that of Eq. (14), or $B_z u_r + d_z \approx C_z Bu^*$. Thus the actual $\dot{z} \approx \dot{z}^*$; consequently, z remains close to z^*, which represents desired performance. Such a u_r can be determined by minimization of the following quadratic function:

$$\min_{u_r} J = \tfrac{1}{2}\big[(1-\varepsilon)(B_z u_r + d_z - C_z Bu^*)^T Q_1 (B_z u_r + d_z - C_z Bu^*) + \varepsilon u_r^T Q_2 u_r\big] \tag{15}$$

for some small $0 < \varepsilon < 1$ and subject to

$$u_{r\,\min} \leq u_r \leq u_{r\,\max} \tag{16}$$

where Q_1 and Q_2 are positive definite matrices of appropriate dimensions. The $u_{r\,\min}$ and $u_{r\,\max}$ in Eq. (16) are the lower and upper bounds of the remaining control surfaces.

The minimization of J subject to Eq. (16) constitutes a QP problem. The term $\varepsilon u_r^T Q_2 u_r$ in Eq. (15) is a regularization term to the QP problem. Without it ($\varepsilon = 0$), the Hessian of J, $\partial^2 J / \partial u_r^2 = B_z^T Q_1 B_z \in R^{m \times m}$, is not strictly positive definite because the rank of $B_z^T Q_1 B_z \in R^{m \times m}$ is at most i but $m > i$. In this case the QP problem has no unique solution, and chattering in u_r can easily occur. On the other hand, any $0 < \varepsilon < 1$ will make the Hessian of J positive definite, and the solution to the QP problem is unique. But clearly ε should be sufficiently small in order for $B_z u_r + d_z - C_z Bu^* \approx 0$. When $B_z u_r + d_z - C_z Bu^* \approx 0$, the response of the aircraft would be very close to that of the healthy aircraft, despite the jamming of a control surface.

B. Analysis

To formalize the preceding heuristic arguments about the rationale of the formulation for control allocation, let us define for given B_z, d_z, and $C_z Bu^*$ the set

$$\mathcal{U} = \{u_r \in R^m \mid B_z u_r + d_z - C_z Bu^* = 0, \quad u_{r\,\min} \leq u_r \leq u_{r\,\max}\} \tag{17}$$

Denote the solution to the QP problem (15) and (16) by $u_r^*(\varepsilon)$ for a given $0 \le \varepsilon < 1$. We first make the following statement:

Property 1

If $\mathcal{U}$ is not empty, the solution u_r^* of the QP problem (15) and (16) has the asymptotic property of

$$\lim_{\varepsilon \to 0} \left[B_z u_r^*(\varepsilon) + d_z - C_z B u^* \right] = 0 \tag{18}$$

When $\varepsilon = 0$, any u_r in $\mathcal{U}$ can be taken to be u_r^*, and $J(u_r^*) = 0$ is the minimum. For $\varepsilon \neq 0$ this claim can be proved by contradiction. Let $\delta_\varepsilon = B_z u_r^*(\varepsilon) + d_z - C_z B u^*$ for a given ε. Suppose that $\delta_\varepsilon \not\to 0$ as $\varepsilon \to 0$. Take an arbitrary $\tilde{u}_r \in \mathcal{U}$. That is, $B_z \tilde{u}_r + d_z - C_z B u^* = 0$, and $J(\tilde{u}_r) = \varepsilon \tilde{u}_r^T Q_2 \tilde{u}_r / 2$. Then for sufficiently small $\varepsilon > 0$, the following will be true:

$$J\left[u_r^*(\varepsilon)\right] = \tfrac{1}{2}\left[(1-\varepsilon)\delta_\varepsilon^T Q_1 \delta_\varepsilon + \varepsilon u_r^{*T}(\varepsilon) Q_2 u_r^*(\varepsilon)\right] > \tfrac{1}{2}\varepsilon \tilde{u}_r^T Q_2 \tilde{u}_r = J(\tilde{u}_r) \tag{19}$$

because $\delta_\varepsilon^T Q_1 \delta_\varepsilon \not\to 0$. But the result that $J[u_r^*(\varepsilon)] > J(\tilde{u}_r)$ contradicts the assumption that u_r^* is the solution of the QP problem. Therefore $\delta_\varepsilon = B_z u_r^* + d_z - C_z B u^*$ must approach zero as $\varepsilon \to 0$. In fact, from the requirement that $J(u_r^*) < J(\tilde{u}_r)$, including the case of sufficiently small $\varepsilon > 0$, we can further conclude that δ_ε must approach zero faster than $\sqrt{\varepsilon}$ as $\varepsilon \to 0$ so that $\lim_{\varepsilon \to 0}[\delta_\varepsilon^T Q_1 \delta_\varepsilon / \varepsilon] \to 0$.

This property formally establishes that we can achieve $B_z u_r + d_z - C_z B u^* \approx 0$ within any practically reasonable accuracy by solving the QP problem with a sufficiently small $\varepsilon > 0$, whenever $B_z u_r + d_z - C_z B u^* = 0$ has solutions within the bounds [Eq. (16)].

Our second claim applies to a more specific case. If rank $(B_z) = i$ (full rank), the equation $B_z u_r + d_z - C_z B u^* = 0$ has infinitely many solutions u_r. But it is well known that the solution defined by the Moore–Penrose pseudoinverse

$$u_{\min}^* = B_z^T \left(B_z B_z^T\right)^{-1} (C_z B u^* - d_z) \tag{20}$$

is the unique one that has the minimum 2-norm $\|\cdot\|^2$ among all such u_r. We state that the solution of the preceding QP problem can be made as close to $u_{\min}^*$ as desired.

Property 2

If the matrix B_z is of full rank and $u_{\min}^*$ defined in Eq. (20) satisfies the constraint (16), then for $Q_2 = I$ and sufficiently small $\varepsilon > 0$ the QP problem (15) and (16) has the solution of

$$u_r^*(\varepsilon) = u_{\min}^* + \eta_\varepsilon \tag{21}$$

where $u_{\min}^*$ is given in Eq. (20), $\eta_\varepsilon \in R^m$ and $\eta_\varepsilon \to 0$ as $\varepsilon \to 0$.

This property can be shown to be true as follows: The assumption that $u_{\min}^*$ satisfies Eq. (16) immediately leads to the conclusion of $u_{\min}^* \in \mathcal{U}$; thus, the set $\mathcal{U}$ is nonempty. By property 1 the solution of the QP problem with small ε can be expressed as $u_r^*(\varepsilon) = \tilde{u}_r + \eta_\varepsilon$ for some $\tilde{u}_r \in \mathcal{U}$ and $\eta_\varepsilon \in R^m$ with $\eta_\varepsilon \to 0$ as $\varepsilon \to 0$. When $Q_2 = I$, the optimal objective function from Eq. (15) becomes

$$J\left(u_r^*\right) = \tfrac{1}{2}\left[(1-\varepsilon)\delta_\varepsilon^T Q_1 \delta_\varepsilon + \varepsilon u_r^{*T} u_r^*\right] = \tfrac{1}{2}\varepsilon\left[(1-\varepsilon)\left(\delta_\varepsilon^T Q_1 \delta_\varepsilon\right)/\varepsilon + \|\tilde{u}_r\|^2 + 2\eta_\varepsilon^T \tilde{u}_r + \|\eta_\varepsilon\|^2\right] \tag{22}$$

where δ_ε is the same as defined in the discussion of property 1. From the observation in the discussion of property 1 that $\lim_{\varepsilon \to 0}(\delta_\varepsilon^T Q_1 \delta_\varepsilon / \varepsilon) \to 0$, clearly for a sufficiently small (but nonzero) ε, the dominant term in $J(u_r^*)$ is $\|\tilde{u}_r\|^2$ because all of the other terms in the brackets approach zero as $\varepsilon \to 0$. For $J(u_r^*)$ to be minimum, $\tilde{u}_r$ must be the one in $\mathcal{U}$ with the minimum 2-norm. Hence $\tilde{u}_r = u_{\min}^*$, where $u_{\min}^*$ is given in Eq. (20).

Property 2 reveals that the QP formulation with $Q_2 = I$ and a small $\varepsilon > 0$ will produce a solution that is practically the same as the commonly employed pseudoinverse solution in control allocation, if such a solution satisfies the constraints (16). But allowing different choices of Q_2 in the QP formulation conveniently provides flexibility to assign preference to small deflections of certain control surfaces, which is not easy to do if the control allocation is only based on enforcing $B_z u_r + d_z - C_z B u^* = 0$.

The preceding discussion confirms formally that the QP formulation with a small ε in Eq. (15) preserves the objective of redistributing u_r to achieve $B_z u_r + d_z - C_z B u^* \approx 0$ whenever it is possible to do within the bounds [Eq. (16)]. When direct control allocation based on solving $B_z u_r + d_z - C_z B u^* = 0$ subject to Eq. (16) is not possible (i.e., the set $\mathcal{U}$ is empty), the solution of the QP problem still provides a best possible u_r.

C. Fixed-Point Iteration Algorithm

A reliable, efficient, and simple algorithm is the key for this control-allocation approach to be practically useful. When none of the constraints in Eq. (16) are active, solving the QP problem is straightforward, and the solution u_r is obtained from the unique solution of the linearalgebraic system $\partial J / \partial u_r = 0$, which gives

$$u_r^* = (1-\varepsilon)\left[(1-\varepsilon)B_z^T Q_1 B_z + \varepsilon Q_2\right]^{-1} B_z^T Q_1 \left(C_z B u^* - d_z\right) \tag{23}$$

In more general cases where some of the constraints in Eq. (16) are active, the standard QP algorithms[8] are more involved and not suited for onboard implementation and applications. But for the special class of QP problems such as in Eqs. (15) and (16) where there are only inequality constraints of the simple form [Eq. (16)], an extremely simple, globally convergent fixed-point iteration algorithm can be devised for onboard use. This method is described and used in Ref. 9 in a different context. Here we shall apply this method to the QP problem (15) and (16).

Define a vector saturator $s[\cdot] = (s_1[\cdot] \cdots s_m[\cdot])^T : R^m \to R^m$ by

$$s_j[\zeta] = \begin{cases} U_j, & \zeta_j \ge U_j \\ \zeta_j, & L_j < \zeta_j < U_j \\ L_j, & \zeta_j \le L_j \end{cases} \qquad j = 1, 2, \ldots, m \tag{24}$$

for any $\zeta = (\zeta_1 \cdots \zeta_m)^T \in R^m$, where for the moment $U_j = u_{\max_j}$ and $L_j = u_{\min_j}$, equal to the upper and lower bound or the jth component of u_r, respectively. Let $H = (1-\varepsilon)B_z^T Q_1 B_z + \varepsilon Q_2$. Calculate the scalar

$$\omega = \left[\sum_{i=1}^{m}\sum_{j=1}^{m} h_{ij}^2\right]^{-\frac{1}{2}} \tag{25}$$

where h_{ij} are the elements of H. Then the solution to the QP problem (15) and (16) satisfies the following fixed-point equation:

$$u_r = s\left[(1-\varepsilon)\omega B_z^T Q_1 \left(C_z B u^* - d_z\right) - (\omega H - I_{m \times m})u_r\right] \triangleq f(u_r) \tag{26}$$

Furthermore, the fixed-point iteration

$$u_r^{(k)} = f\left[u_r^{(k-1)}\right], \qquad k = 1, 2, \ldots, \qquad \forall u_r^{(0)} \in R^m \tag{27}$$

converges to the unique solution of the QP problem from any initial guess $u_r^{(0)}$.

The validity of this fixed-point algorithmis established by examining the necessary and sufficient conditions for the QP problem and using global contraction mapping theory.[9] The unconstrained solution (23) is just a special case of Eq. (26) when none of the components of the saturator s in Eq. (26) are active. In such a case $s[\zeta] = \zeta$; therefore, Eq. (26) simply reduces to Eq. (23). But it should be stressed that in general, the QP problem solution by Eq. (26) is different from what is obtained by clipping off (saturating) the right-hand side of Eq. (23).

The fixed-point iteration algorithm (27) is particularly suited for onboard implementation. If the initial guess $u_r^{(0)}$ is chosen to be the solution of the QP problem in the preceding control update cycle, the current u_r should be obtained in just a few iterations from Eq. (27).

A similar constrained optimization problem was formulated in Ref. 2 for redistributing control surfaces after the failure. Although simulations showed good performance, the computation requirement using a standard optimization algorithm was deemed to be too

intensive for onboard implementation. Another concern was about the convergence rate. These concerns appear to be satisfactorily addressed by the current algorithm.

Finally, this method can be easily modified to accommodate both control surface amplitude and rate constraints. Suppose, in addition to the amplitude constraint (16) that the rate limit for the jth surface is $\dot{u}_{\max_j}$, and the sampling time of the control system is Δt. The only modifications will be to redefine the bounds of the saturator [Eq. (24)] at each t by

$$U_j = \min\{u_{\max_j},\ \Delta t \dot{u}_{\max_j} + u_j(t - \Delta t)\} \tag{28}$$

$$L_j = \max\{u_{\min_j},\ -\Delta t \dot{u}_{\max_j} + u_j(t - \Delta t)\} \tag{29}$$

where $u_j(t - \Delta t)$ is the calculated control command for u_j at the earlier update.

IV. Reconfigurable Entry Flight-Control Designs for the X-33

A brief description of the X-33 vehicle and its flight-control system has been given in the Introduction. The X-33 vehicle relies on engine thrust vectoring and aerosurfaces during the ascent phase. During the entry phase, the X-33 will be controlled by aerosurfaces and reaction control jets. During the ascent phase, only marginal benefits of reconfiguration were shown because of the corrective forces of which the engine thrust vectoring is capable can overcome any failed surface position. This study presents the results for the entry phase because control reconfiguration has been shown to have the greatest payoff during entry. The Appendix provides the linearized dynamic model at a critical entry condition of Mach 3.16. This operating point will be used to demonstrate the two design approaches introduced in the preceding sections because this flight condition is a critical, unstable lateral-directional point. Both the longitudinal and lateral-directional time histories will be shown because of coupling between axes following a surface failure.

Once the control laws were designed, they were implemented in a high-fidelity nonlinear six-degree-of-freedom simulator for the X-33. Unless indicated otherwise, all of the simulation results presented in this paper were from the nonlinear simulation.

A. Determination of Trimmable Jam Positions

Before proceeding with the reconfigurable control design, it is helpful to understand whether the vehicle can still be retrimmed with a particular aerosurface jammed at a given position. Rewrite the postfailure aircraft model as

$$\dot{x} = Ax + B_r u_r + b_\delta \delta \tag{30}$$

where as before δ is the jammed surface position, B_r is the postfailure B matrix, u_r the remaining control surfaces, and b_δ the sensitivity vector corresponding to the jammed surface. Let y_{test} represent the three body angular (roll, yaw, and pitch) rates in the body frame. Suppose that $y_{\text{test}} = C_{\text{test}} x$. Clearly

$$\dot{y}_{\text{test}} = C_{\text{test}} Ax + C_{\text{test}} B_r u_r + C_{\text{test}} b_\delta \delta \tag{31}$$

A necessary condition for retrimming the vehicle with the jammed surface is that the right-hand side of the preceding equation can still be made to vanish at $x = 0$ with a u_r in its allowable range. To find the range of jammed positions of the surface δ for which retrim is possible, we may solve the following linear programming (LP) problem

$$\min_{u_r,\delta} \delta \quad (\text{or} \max_{u_r,\delta} \delta) \tag{32}$$

subject to

$$C_{\text{test}} B_r u_r + C_{\text{test}} b_\delta \delta = 0 \tag{33}$$

$$u_{r\min} \le u_r \le u_{r\max}, \qquad \delta_{\min} \le \delta \le \delta_{\max} \tag{34}$$

The solution of the LP problem (32–34) gives the minimum (most negative) or maximum jammed incremental position of δ that can be balanced at the trim condition by the remaining aerosurfaces u_r within their deflection limits. This range found serves as a reasonable estimation of the limits within which the reconfigurable control system can still possibly stabilize the vehicle. In some cases including α, β, and v in y_{test} can give a more accurate estimate because the balance of forces is considered this way as well.

Applying this technique to the X-33 model in the Appendix, we found that for any jammed position within the physical limits of all aerosurfaces but the flaps the vehicle can always be retrimmed. For a jammed body flap, however, it was found that $\delta_{\min} = -18.9$ (deg) and $\delta_{\max} = 10.$ (deg) (incremental from the trim position). This is because the body flaps are the predominant aerosurfaces for pitch control, and other aerosurfaces cannot adequately compensate for

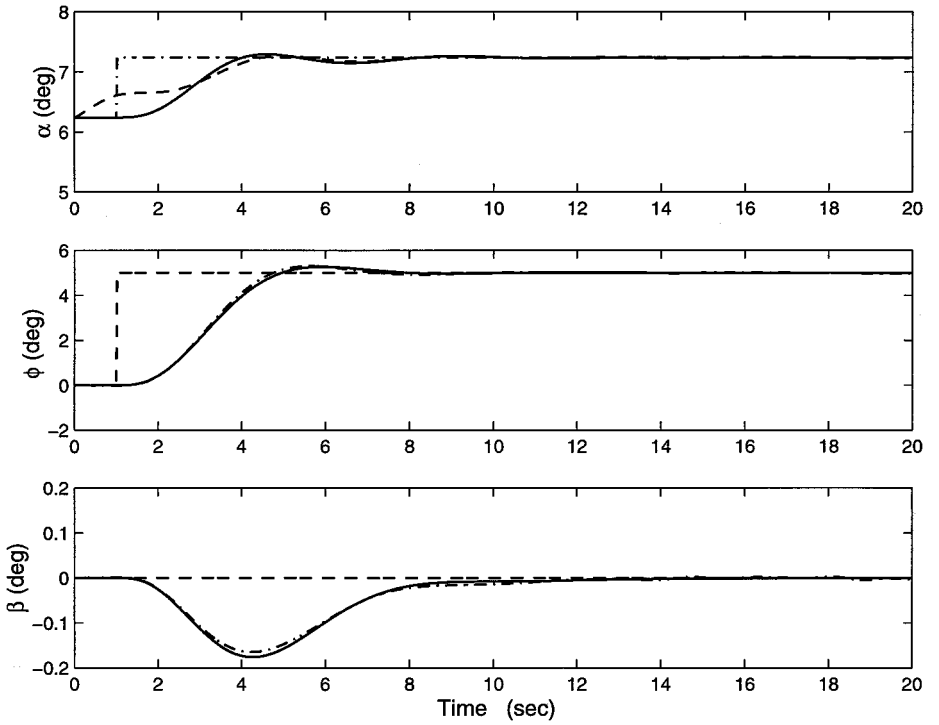

Fig. 2a X-33 response from the linearized model (——) and nonlinear simulation (– – –).

it if one of the flaps is jammed at a position far from their trim positions. When there are commands to be tracked, the range of recoverable body flap jammed positions will likely be even smaller than the range just found because tracking of the commands requires additional deflections of the remaining aerosurfaces. Also, because the preceding analysis is based on the linearized model, the actual trimmable limits based on the nonlinear model can be different to certain extent.

B. Servomechanism Reconfigurable Design

Following the method in Sec. II, we can design a PI-reconfigured control system for the jam of each surface. The gains of all eight such controllers will be stored onboard. Should the jam occur inflight, based on the information provided by the EMAs, an appropriate reconfigured controller will be switched on. The three outputs to be commanded are ϕ (roll angle), β (sideslip angle), and α (angle of attack). The β command is normally zero for coordinated flight. Although the linearized longitudinal and lateral directional dynamics are decoupled in the system matrix A, all of the control surfaces contribute to both longitudinal and lateral dynamics at different extents. Therefore the control design is carried out simultaneously for both directions. In design of the feedback PI control law, the forward velocity is ignored because it has negligible effect on the response. Assume constant commands ϕ_{cmd}, β_{cmd}, and α_{cmd}. With

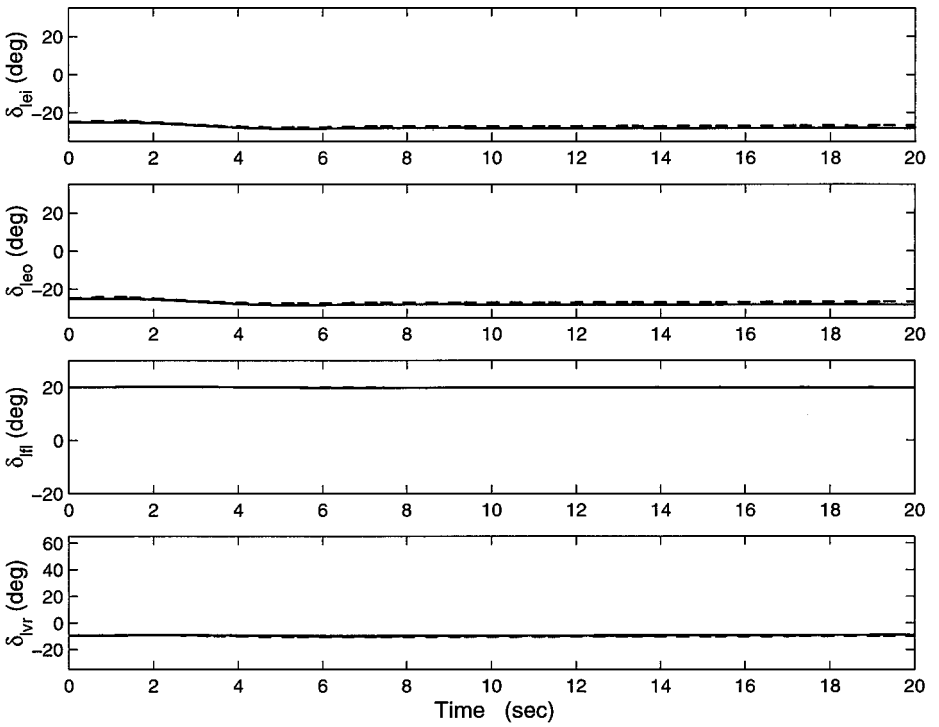

Fig. 2b Comparison of response from linearized model (——) and nonlinear model (– – –) for the left-side control surfaces.

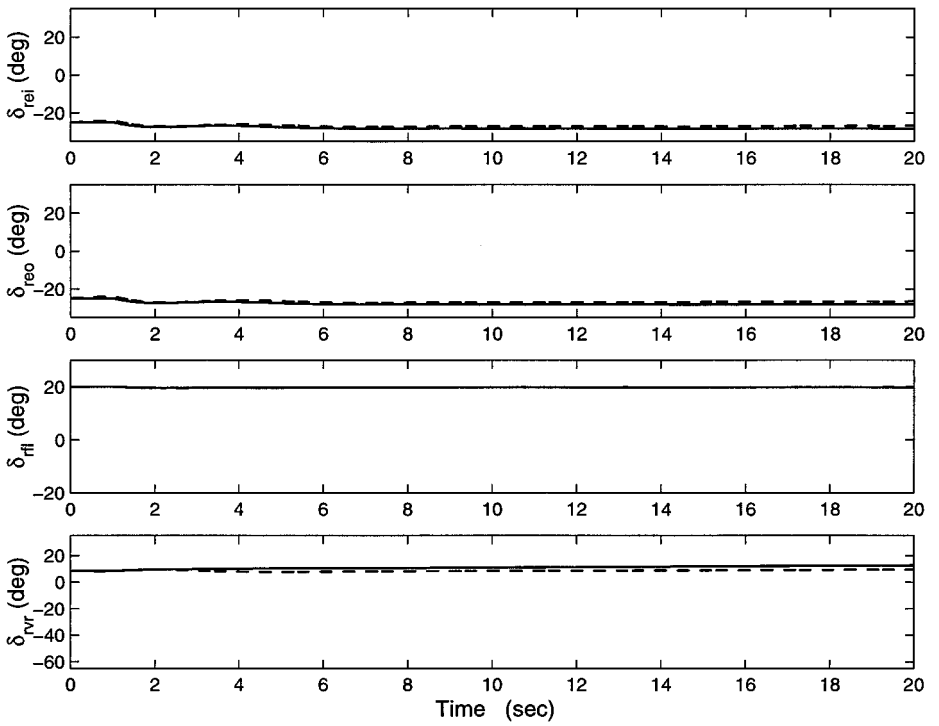

Fig. 2c Comparison of response from linearized model (——) and nonlinear model (– – –) for right-side control surfaces.

$y = (\phi\ \beta\ \alpha)^T$ and $r = (\phi_{\text{cmd}}\ \beta_{\text{cmd}}\ \alpha_{\text{cmd}})^T$, the controller dynamics (5) are now

$$\dot{x}_{c1} = \phi_{\text{cmd}} - \phi, \qquad \dot{x}_{c2} = \beta_{\text{cmd}} - \beta, \qquad \dot{x}_{c3} = \alpha_{\text{cmd}} - \alpha \tag{35}$$

For each jammed surface the remaining seven surfaces and the eight vehicle states (excluding the forward velocity) plus the three integrators states [Eqs. (35)] constitute the augmented system (8). This augmented system is found to be controllable. An LQR control law for the augmented system, which is a PI control law for the X-33 in the form of

$$u_r = K_x x + k_\phi \int (\phi_{\text{cmd}} - \phi)\,\mathrm{d}t + k_\beta \int (\beta_{\text{cmd}} - \beta)\,\mathrm{d}t + k_\alpha \int (\alpha_{\text{cmd}} - \alpha)\,\mathrm{d}t \tag{36}$$

can be easily designed, where $x = (p\ r\ \beta\ \phi\ \psi\ \alpha\ q\ \theta)^T$. We have found that for each jammed surface, except for the flaps, a single set of gains are adequate to handle any jammed position within its deflection limits. No scheduling of the gains with respect to the jammed position is necessary. For a jammed flap a single set of gains are adequate to restabilize the X-33 for jammed flap in a retrimmable

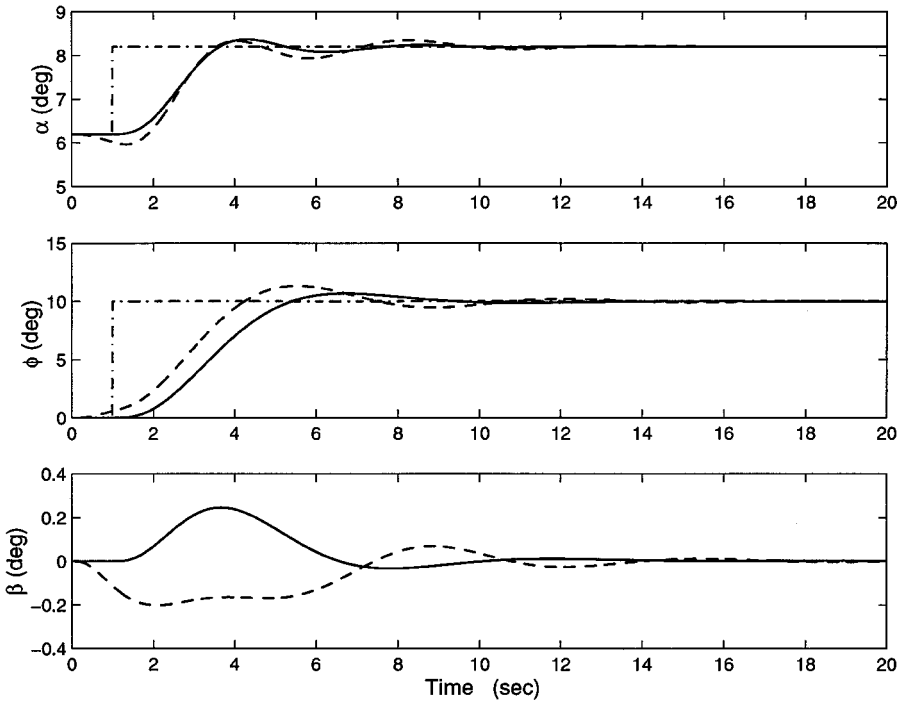

Fig. 3a Comparison of responses using PI-servo method with left inboard elevon runaway then jammed at −15 deg (– – –) and nominal controller without a failure (——).

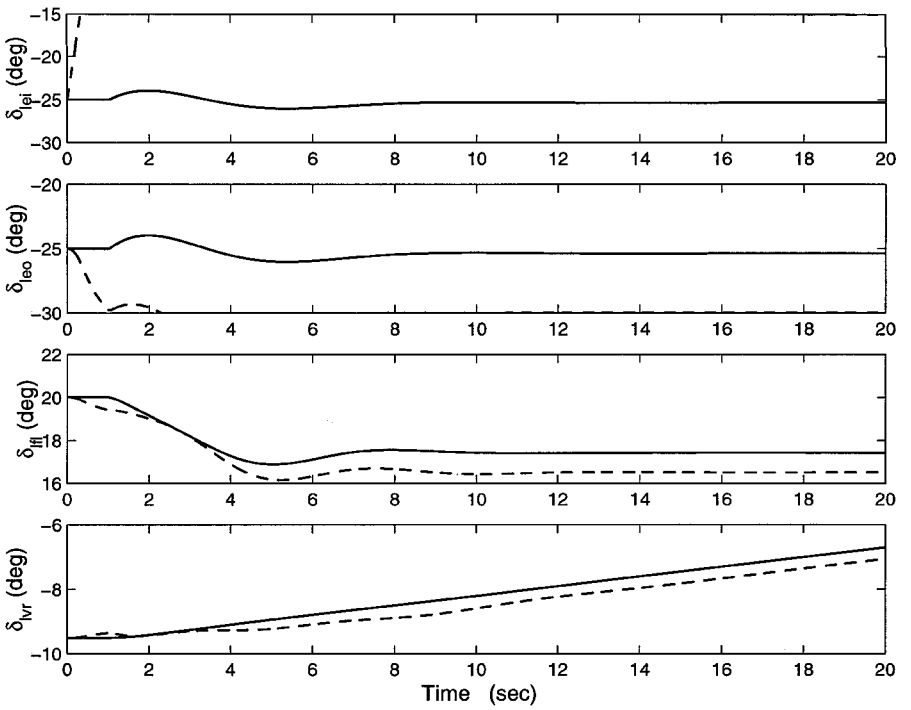

Fig. 3b Comparison of responses using PI-servo method with left inboard elevon runaway then jammed at −15 deg (– – –) and nominal controller without a failure (——) for left-side control surfaces.

position (cf., Sec. IV.B). This range cannot be increased by any gain scheduling with respect to the jammed flap position because this is the physical limit for the X-33 to be able to retrim.

Figures 2a–2c show a time history comparison of the linearized model and the nonlinear six-degree-of-freedom simulator for the X-33 under the same control law. The results show a good comparison between the linear model and the six-degree-of-freedom simulation. No gain adjustments were made in this case and in the following cases when applying the control law to the nonlinear simulator. Even though these results matched, when using a linear model (linear plant and simple nonlinear actuators with rate limits and surface saturation limits) special attention must be taken when analyzing control effector activity or actuator response, especially for reconfiguration design. It is recommended that a high-fidelity nonlinear simulator be used to validate the linear design results. For the remaining position of the paper, the time-history results are from the nonlinear six-degree-of-freedom simulator.

Figures 3a–3c show how the servomechanism controller with a failure works compared to the nominal case without a failure. These figures in dashed line show the time histories of a runaway left inboard elevon failure that starts at $t = 0$ and jams at -15 deg. A longitudinal and lateral-directional guidance command tracking

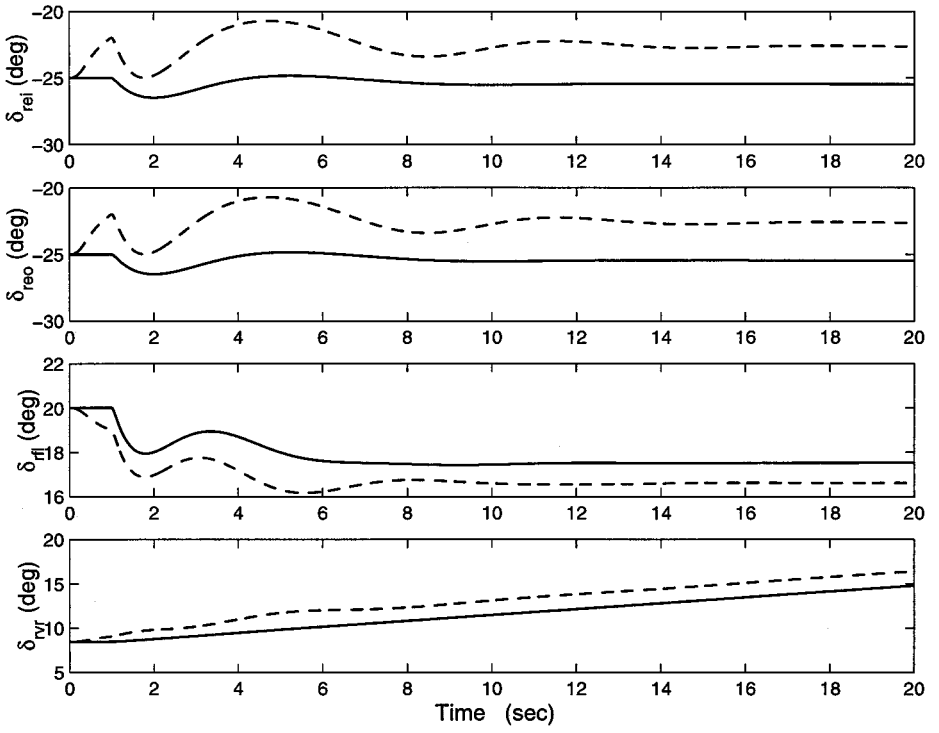

Fig. 3c Comparison of responses using PI-servo method with left inboard elevon runaway then jammed at − 15 deg (- - -) and nominal controller without a failure (——) for right-side control surfaces.

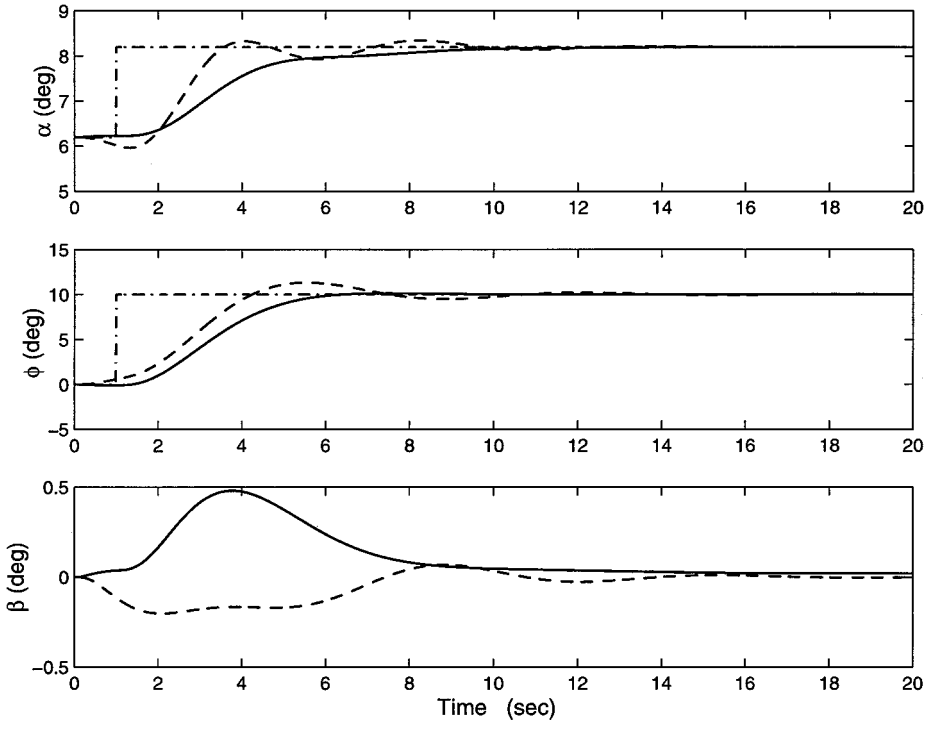

Fig. 4a Comparison of responses using PI-servo method with left inboard elevon runaway then jammed at − 15 deg (- - -) and control-allocation method (——).

step input starts at $t = 1$. The guidance commands are for simultaneous tracking of angle-of-attack and roll-angle commands during the failure because maneuvers in both axes are more demanding of the reconfigurable control system. Sideslip angle command remains at 0.0 deg for all test cases. Figure 3a shows the commands and the resulting responses. The PI-servo controller tracks the commanded angle of attack of 8 deg and the roll angle of 10 deg adequately. Figure 3b shows the left surface positions, and Figure 3c shows the right surface positions. As can be seen in these figures, the servomechanism controller with a failure performs almost as well as the nominal controller without a failure.

This servomechanism control approach was found to work well for any jammed positions of any of the six aerosurfaces, excluding the flaps. For the jamming of one of the flaps not far from the trim position, the PI control system still performs well. Only when a flap is jammed at a position far from its trim position, the performance of the reconfigured PI control system begins to degrade considerably.

C. Control-Allocation Reconfigurable Design

A reference PI control law using all of the eight aerosurfaces of the healthy X-33 is designed using the servomechanism and LQR method to serve as the baseline control law

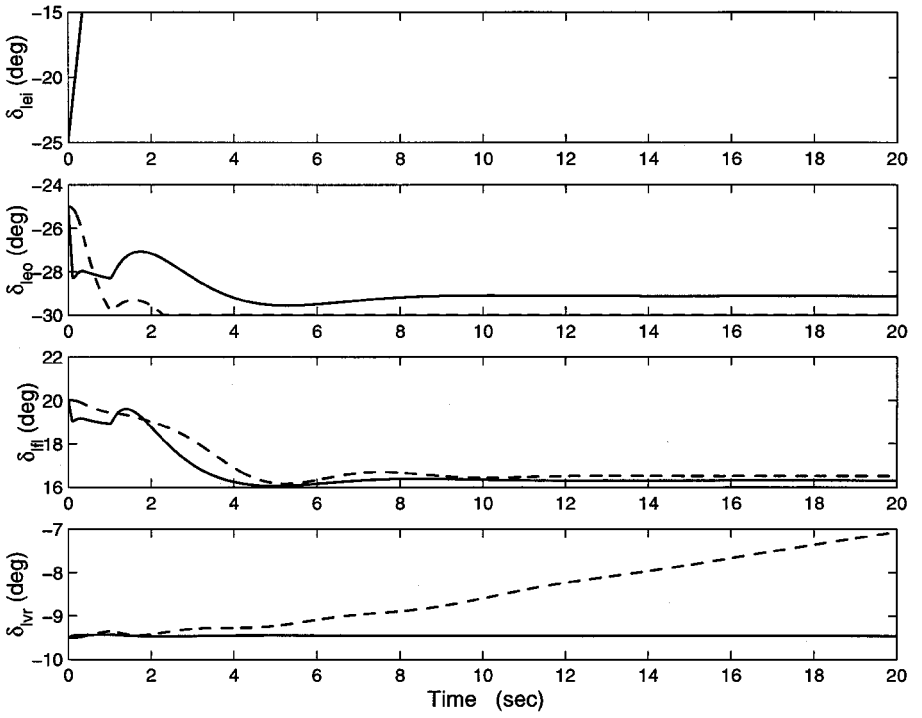

Fig. 4b Comparison of responses using PI-servo method with left inboard elevon runaway then jammed at −15 deg (– – –) and control-allocation method (——) for left-side control surfaces.

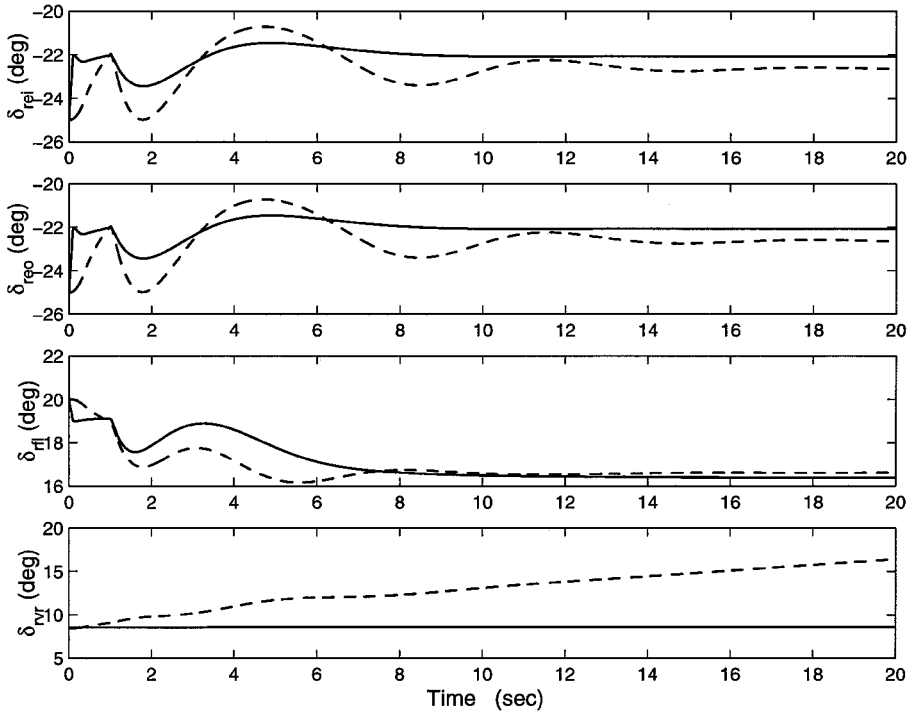

Fig. 4c Comparison of responses using PI-servo method with left inboard elevon runaway then jammed at −15 deg (– – –) and control-allocation method (——) for right-side control surfaces.

$$u^* = K_x^* x + k_\phi^* \int (\phi_{\text{cmd}} - \phi)\,\mathrm{d}t + k_\beta^* \int (\beta_{\text{cmd}} - \beta)\,\mathrm{d}t + k_\alpha^* \int (\alpha_{\text{cmd}} - \alpha)\,\mathrm{d}t \tag{37}$$

The reference control law should not push the vehicle too hard for performance. Otherwise the vehicle after failure may not be able to generate the control actions the reference controller calls for. This would be the case when the set $\mathcal{U}$ in Eq. (17) is empty, and if this happens too frequently, instability could occur.

The controlled output vector z used in Sec. III is chosen to be $z = (p\ r\ q\ \beta\ \alpha)^T = C_z x$. The β and α are added to z, in addition to p, r, and q, because they are part of the commanded outputs of the X-33. But the difference in term of the response as compared to the case where $z = (p\ r\ q)^T$ was found to be indiscernible.

For each jammed surface the reference u^* is always computed from Eq. (37) at the current state x. The Q_1 and Q_2 matrices in Eq. (15) are chosen to be identity matrices, and $\varepsilon = 0.0005$ is used. The control commands for the remaining seven aerosurfaces are obtained from the fixed-point iteration (27).

Figure 4a shows the performance comparison of the control-allocation approach and the servo-PI controller for the case of a runaway left inboard that jams at −15 degs (see Fig. 3). Figures 4b and 4c depict the aerosurface variations for both methods. The results

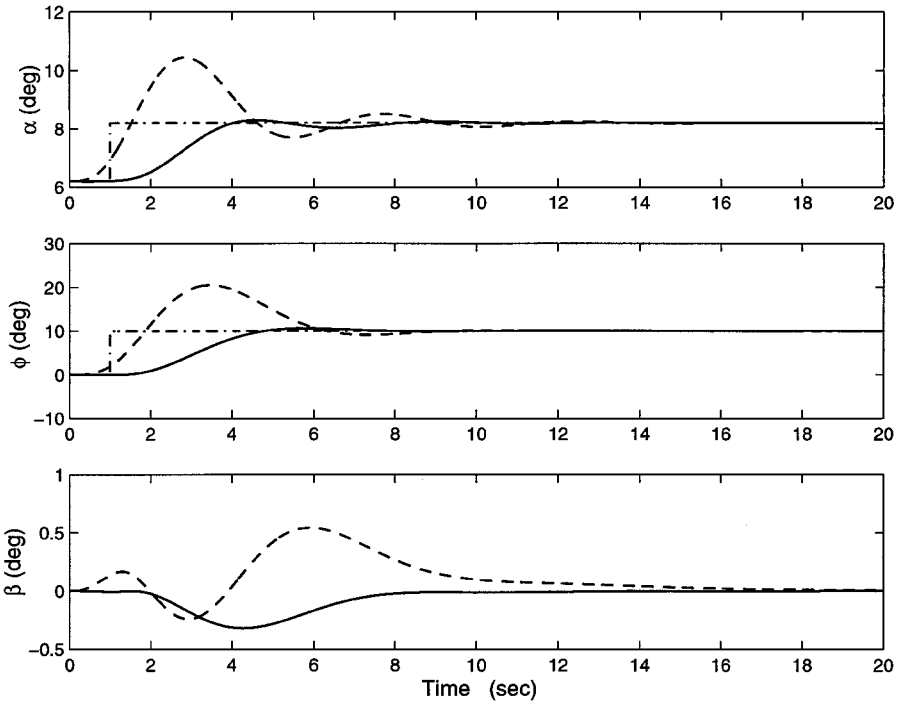

Fig. 5a Comparison of responses using PI-servo method with right body flap runaway then jammed at 10 deg (– – –) and control-allocation method (——).

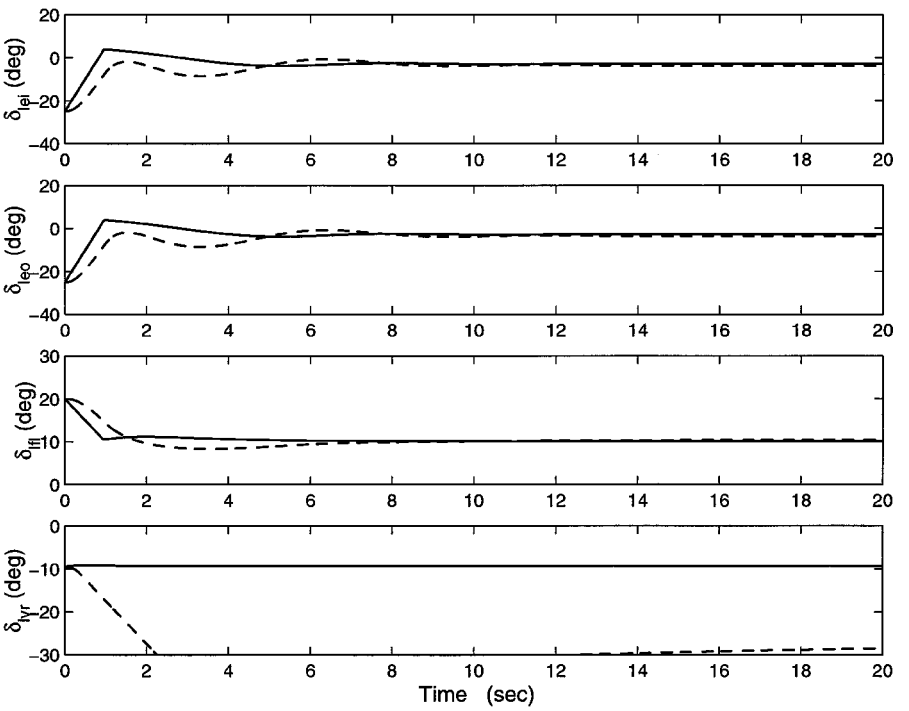

Fig. 5b Comparison of responses using PI-servo method with right body flap runaway then jammed at 10 deg (– – –) and control-allocation method (——) for left-side control surfaces.

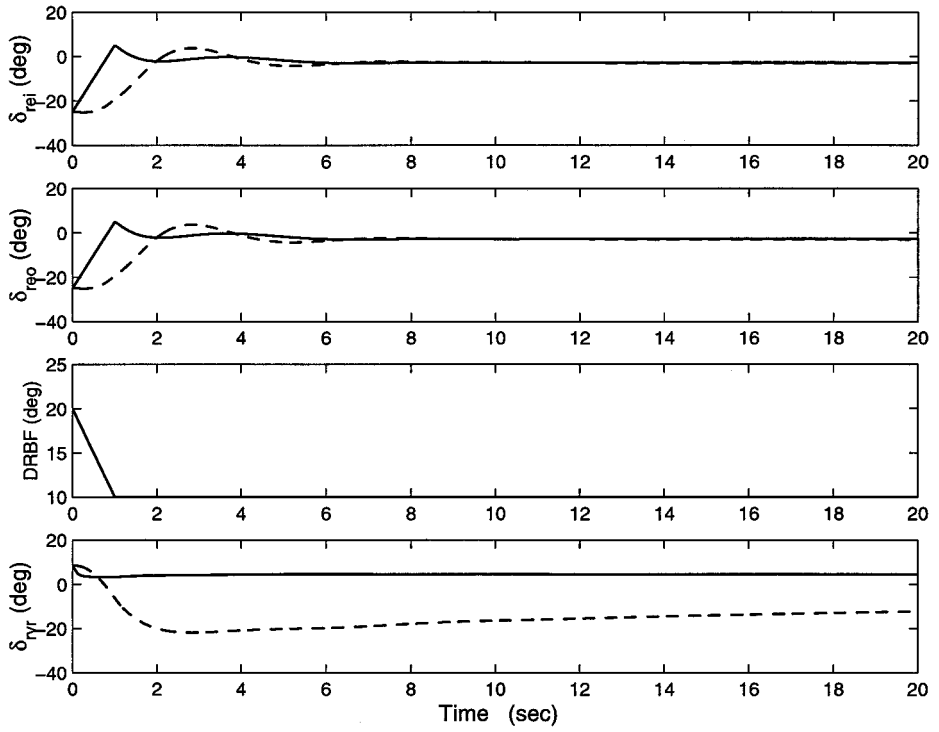

Fig. 5c Comparison of responses using PI-servo method with right body flap runaway then jammed at 10 deg (– – –) and control-allocation method (——) for right-side control surfaces.

show that the servo-PI controller has some overshoot, whereas the control-allocation method was well damped with low control surface activity (Figs. 4b and 4c).

Figure 5a shows the performance comparison of the control-allocation approach and the servo PI controller for a runaway right body flap from 20 to 10 deg. Figures 5b and 5c show the control surface positions for both methods. The control-allocation approach provided a good response in this and other similar difficult cases, whereas the servo-PI method did not have as good a performance. A tradeoff here is that the control-allocation method needs to know the surface and position that has failed, but the servo-PI method only needs to know what surface failed, not the position.

The responses seen in Figs. 4a and 5a under the control-allocation reconfiguration are similar. In fact, the control-allocation approach is found to provide uniformly good performance for all of the failure (jamming) cases where stabilization and command-tracking are possible with the remaining aerosurfaces. Especially in the challenging situations where a body flap is jammed, the control-allocation approach yields nearly the same good performance for any jammed position of a body flap within the retrimmable range. When the flap jammed position is outside the retrimmable range, instability occurs rapidly because some of the remaining operable surfaces become severely saturated when trying to counter the jammed flap.

V. Conclusions

Two methods for design of reconfigurable flight-control systems to handle jammed control surface are presented. One is based on a robust servomechanism design methodology. For the failure cases of jammed surface, the approach leads to a MIMO PI controller. The other method uses a QP-based control-allocation scheme to redistribute the operable control surfaces to cancel the influence of the jammed surface and still provide desired control moments and forces to the aircraft. The formulation is formally analyzed to justify its validity, and a globally convergent, simple fixed-point algorithm is developed for onboard implementation of the method. The servo-PI controllers are simple to implement, and the position of the failed surface need not be known. But a different controller is needed for each possible jammed surface. The control-allocation method on the other hand requires no separate designs for different jammed surfaces, but modest online computation and adequate control redundancy are needed. The control allocation does require the knowledge of the jammed position of the failed surface. Therefore the answer to the question of which design is more suitable depends on the onboard resources.

Applications of both approaches to reconfigurable entry flight control of the X-33 vehicle demonstrate the potential of the two methods. The servo-PI controller provides good performance in all but the most severe failure scenarios. In comparison, uniformly good and virtually the same performance is achieved by the control-allocation-based controller, regardless of which surface is jammed, as long as it is still possible to control the vehicle within the authority of the remaining surfaces.

Although only one jammed control surface is discussed throughout this work, it is straightforward to extend the two methods introduced here to the cases where jam of more than one surface occurs if the consideration of such an event is warranted.

Finally, we recognize that reconfigurable control design methods exist that can be applied to more general failure scenarios and are better suited to handle nonlinearity.[1,4] But the methods discussed in this paper are consistent with the current framework of how flight control systems are designed and appear to be very effective for the restricted class of failures (jammed surfaces). A reconfigurable flight-control system designed with these methods can be easily evaluated and tested in accordance with today's well-established criteria and standards. This may prove to be important for the methods to gain acceptance in practice.

Appendix: Linearized Model of the X-33

The following is a linearized model of the X-33 near the terminal area energy management interface in entry flight. The flight conditions are Mach = 3.16, height = 97,167 ft, $\alpha_{\text{trim}} = 6.23$ deg, $\theta_{\text{trim}} = 0.922$ deg, $\phi_{\text{trim}} = \beta_{\text{trim}} = 0$, and weight = 78,593 lbm. Let $u = (\delta_{\text{rei}}\ \delta_{\text{lei}}\ \delta_{\text{rfl}}\ \delta_{\text{lfl}}\ \delta_{\text{rvr}}\ \delta_{\text{lvr}}\ \delta_{\text{reo}}\ \delta_{\text{leo}})^T$ be the control surface perturbations from the trim values, where δ_{rei}, δ_{lei} are the right and left inboard elevons, δ_{rfl}, δ_{lfl} the right and left body flaps, δ_{rvr}, δ_{lvr} the right and left rudders, and δ_{reo}, δ_{leo} the right and left outboard elevons.

All of the control-surface deflections are in degrees. The sign convention is positive body flap deflection is down, positive elevon deflection is down, and positive rudder delection is left looking forward. The surface trim values are 19.98 deg for the body flaps,

−24.88 deg for the inboard and outboard elevons, and 9.4 deg for the right rudder and −9.43 deg for the left rudder. Let the perturbations from the trim conditions be $x = (p\ r\ \beta\ \phi\ \psi\ \alpha\ q\ \theta\ v)^T$, where the components are, in the order of appearance in x, roll rate, yaw rate, sideslip angle, roll angle, yaw angle, angle of attack, pitch rate, pitch angle, and forward velocity. The units are in degrees/second for angular rates, degrees for angles, and feet/second for velocity. The linearized dynamics of the X-33 at the preceding flight conditions are given by

$$\dot{x} = Ax + Bu \tag{A1}$$

where

$$A = \begin{bmatrix} A_{\text{lat}} & 0 \\ 0 & A_{\text{lon}} \end{bmatrix} \tag{A2}$$

with

$$A_{\text{lat}} = \begin{bmatrix} -0.099170 & 0.020570 & 2.805001 & 0.000001 & 0.000001 \\ -0.002640 & -0.031920 & -0.674200 & 0 & 0 \\ -0.108500 & -0.994000 & -0.029750 & 0.010210 & 0.000034 \\ 1.0 & 0.016090 & -0.000148 & 0.000016 & 0 \\ 0 & 1.0 & 0.000120 & -0.000013 & 0.000122 \end{bmatrix} \tag{A3}$$

$$A_{\text{lon}} = \begin{bmatrix} -0.064190 & 1.000001 & 0.000884 & -0.000130 \\ -1.424000 & -0.051730 & 0.000001 & 0 \\ -.0000138 & 1.0 & 0.000014 & 0.000003 \\ -0.550041 & 0 & -0.559090 & -0.013375 \end{bmatrix} \tag{A4}$$

$$B = \begin{bmatrix} -0.2883 & 0.2883 & -0.8654 & 0.8654 & -0.0000 & 0.0025 & -0.2883 & 0.2883 \\ -0.0959 & 0.0959 & 0.2079 & -0.2079 & -0.0045 & -0.0051 & -0.0959 & 0.0959 \\ 0.0000 & 0.0000 & 0.0003 & -0.0003 & -0.0001 & 0 & 0 & 0 \\ 0 & 0 & 0 & 0 & 0 & 0 & 0 & 0 \\ 0 & 0 & 0 & 0 & 0 & 0 & 0 & 0 \\ -0.0005 & -0.0005 & -0.0019 & -0.0019 & -0.0005 & 0.0004 & -0.0005 & -0.0005 \\ -0.0857 & -0.0857 & -0.5263 & -0.5263 & 0.0098 & -0.0073 & -0.0857 & -0.0857 \\ 0 & 0 & 0 & 0 & 0 & 0 & 0 & 0 \\ -0.0034 & -0.0034 & -0.1285 & -0.1285 & 0.0011 & -0.0011 & -0.0041 & -0.0041 \end{bmatrix} \tag{A5}$$

Note that the A matrix is decoupled in the longitudinal and lateral directions, but the B matrix is not.

Acknowledgment

The authors at Iowa State University gratefully acknowledge the support for this research by the NASA Dryden Flight Research Center under Corporative Agreement NCC4-117.

References

[1]Brinker, J. S., and Wise, K. A., "Reconfigurable Flight Controls for a Tailless Advanced Fighter Aircraft," *Proceedings of Guidance, Navigation, and Control Conference*, Vol. 1, AIAA, Reston, VA, 1998, pp. 75–87.

[2]Wagner, E., Burken, J., Hanson, C., and Wohletz, J., "Deterministic Reconfigurable Control Design for the X-33 Vehicle," *Proceedings of Guidance, Navigation, and Control Conference*, Vol. 3, AIAA, Reston, VA, 1998, pp. 1342–1351.

[3]Morse, W. D., and Ossman, K. A., "Model Following Reconfigurable Flight Control System for the AFTI/F-16," *Journal of Guidance, Control, and Dynamics*, Vol. 13, No. 6, 1990, pp. 969–976.

[4]Calise, A. J., Lee, S., and Sharma, M., "Direct Adaptive Reconfigurable Control of a Tailless Fighter Aircraft," *Proceedings of Guidance, Navigation, and Control Conference*, Vol. 1, AIAA, Reston, VA, 1998, pp. 88–97.

[5]Desoer, C. A., and Wang, Y. T., "Linear Time-Invariant Robust Servomechanism Problem: A Self-Contained Exposition," *Control and Dynamic Systems*, edited by C. T. Leondes, Vol. 16, Academic, New York, 1980, pp. 81–129.

[6]Davison, E. J., "The Robust Control of a Servomechanism Problem for Linear Time-Invariant Multivariable Systems," *IEEE Transactions on Automatic Control*, Vol. AC-21, No. 1, 1976, pp. 25–34.

[7]Enns, D., "Control Allocation Approaches," *Proceedings of Guidance, Navigation, and Control Conference*, Vol. 1, AIAA, Reston, VA, 1998, pp. 98–108.

[8]Luenburger, D. G., *Linear and Nonlinear Programming*, 2nd ed., Addison Wesley Longman, Reading, MA, 1984, pp. 425, 426.

[9]Lu, P., "Constrained Tracking Control of Nonlinear Systems," *Systems and Control Letters*, Vol. 27, 1996, pp. 305–314.